ACS APPLIED MATERIALS & INTERFACES
Research Article
www.acsami.org

Enhanced Electrical Properties of Thin-Film Transistor with Self-Passivated Multistacked Active Layers

Deuk Jong Kim, You Seung Rim, and Hyun Jae Kim*

School of Electrical and Electronic Engineering, Yonsei University, 50 Yonsei-ro, Seodaemun-gu, Seoul 120-749, Korea

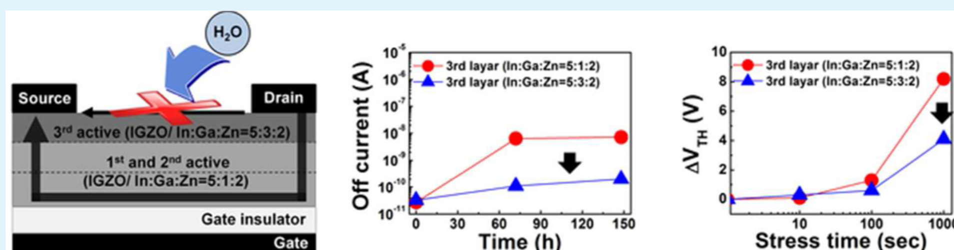

ABSTRACT: To enhance the solution-processed thin-film transistor (TFT) performance, we proposed a TFT with self-passivated multistacked active layers (SP-MSALs). This structure exhibited self-protection in the active layer as compared with the conventional TFT structure. The self-passivation layer prevented the leakage current path at the back-channel region, thus improving the field-effect mobility (μ_{FET}) and the positive bias stress (PBS) reliability. In addition, it was very stable in the exposed environment even for 150 h. As a result, the proposed SP-MSAL TFT caused the threshold voltage shift (ΔV_{TH}) under PBS to improve from 8.2 to 4.2 V as compared with the conventional MSAL TFTs.

KEYWORDS: *Solution process, metal oxide semiconductor, multilayer, self-passivation layer, time stability*

1. INTRODUCTION

Recently, the realization of high-performance and low-temperature processing of solution-processed oxide semiconductors have attracted attention and have been studied for high-pressure annealing,[1] UV annealing,[2] and synthesis of novel solutions.[3,4] These solution-processed oxide semiconductors have many advantages in terms of a nonvacuum process, selective deposition, and so on.[5,6] Accordingly, the solution-processed oxide semiconductor-based thin-film transistor (TFT) can be grafted not only onto the next-generation display but also onto a functional integrated circuit at low cost.[7] However, the solution-processed films suffer from some problems such as a large number of defects because of the porosity of the film, which seriously hinders high-performance realization.[8,9] Earlier, we reported that the electrical performance such as field-effect mobility (μ_{FET}) and positive bias stress (PBS) reliability improved by introducing three-stacked active layers (3-SALs) to the solution-processed TFT.[9] However, the 3-SAL TFTs suffered from a problem where the off-current increased, attributed to the absorbed water on the back surface when they were stored in an ambient environment for some periods. This phenomenon is due to the absence of a passivation layer that protects the ambient gases. In the absence of the passivation layer, reliability worsens.[10,11] To avoid this problem, we proposed methods of providing a protection layer, e.g., N_2O plasma treatment of the back surface and formation of a nitrogenized amorphous IGZO.[19−22] However, these methods required additional processes after the construction of the active layer. In this paper, an experiment was performed to assign the passivation function to the third layer of the 3-SAL to solve this problem. Therefore, we propose the self-passivated multistacked active layers (SP-MSALs) to improve the reliability of the solution-processed TFT.

2. EXPERIMENTAL PROCEDURE

IGZO solution was prepared by dissolving indium nitrate hydrate [$In(NO_3)_3 \cdot xH_2O$], gallium nitrate hydrate [$Ga(NO_3)_3 \cdot xH_2O$], and zinc acetate [$Zn(CH_3COO)_2 \cdot 2H_2O$] in a 20 mL of 2-methoxyethanol. Monoethanolamine and acetic acid (CH_3COOH) were added to improve the solubility and to prepare a homogeneous solution, respectively. The total concentration of In, Ga, and Zn precursor was 0.1 M. The In:Zn mole ratio was fixed at 5:2. The Ga/(In + Ga + Zn) ratio was varied at 0%, 13%, 30%, and 42%. To fabricate the bottom-gate TFTs, the prepared IGZO solutions were spin coated at 3000 rpm for 30 s in a heavily doped p-type Si substrate with a 1200-Å-thick SiO_2 layer. To fabricate the 3-SAL TFTs, the spin coating and pre- and postannealing processes were repeated three times. The pre- and postannealing processes were performed for 5 min at 300 °C and for 1 h at 450 °C, respectively. In particular, the SP-MSALs were stacked at the third layer by the IGZO solution (In:Ga:Zn = 5:x:2, where x = 0, 1, 3, and 5) and on the first and second layers by the IGZO solution (In:Ga:Zn = 5:1:2). After postannealing, 200-nm-thick aluminum (Al) sputtered with a shadow mask was used as the source and drain electrodes. The width and length of the channel were 1000 and 150 μm, respectively. The resistivity and the carrier concentration of the IGZO films were analyzed by the Hall effect measurement. To analyze the chemical binding of the oxygen vacancies, X-ray photoelectron spectroscopy (XPS) was performed. The electrical properties were

Received: January 27, 2013
Accepted: April 17, 2013
Published: April 17, 2013

© 2013 American Chemical Society

measured, which induced a gate voltage (V_G) from −30 to 30 V and a drain voltage (V_D) of 10 V. The positive bias stress (PBS) condition was characterized by a V_G of 20 V and a V_D of 10 V, applied for 1000 s. To evaluate the change in the off-current level with time, we measured the transfer characteristics after storing the TFTs at ambient air.

3. RESULTS AND DISCUSSION

3.1. Electrical Characteristics of IGZO TFTs with Single Active Layer by Varying the Ga Mole Ratio. In our previous research, we reported that the reliability features of μ_{FET} and the PBS improved through the use of TFTs with 3-SALs.[9] However, when the fabricated device was kept in open air for a long time and revaluated, the off-current increased, as shown in Figure 1a. Figure 1b shows that the TFT was affected by the absorbed water molecules in the back channel. The leakage current, which was not controlled by the gate voltage, flowed through the back-channel region.[10] To solve this problem, we performed an experiment, which changed the electrical properties of the third layer of the 3-SALs exposed to the outside environment so that it can assume the characteristics of a protection layer. Here, we focused on the role of Ga among the IGZO elements. Because Ga has high electron affinity and strong attraction to oxygen ions, it can reduce the carrier concentration because of the decrease in the oxygen vacancies as well as reduce the trap sites related to the oxygen vacancies.[11−13]

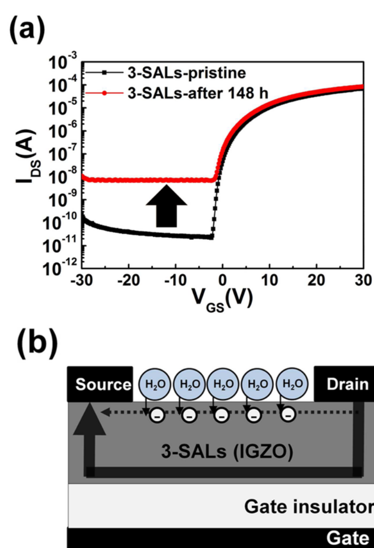

Figure 1. Problem of TFTs without passivation layer (increasing the off-current in the air environment). (a) Transfer characteristics of the 3-SAL TFTs with time. (b) Schematic diagrams of the increase in the off-current.

To investigate the characteristics of the single IGZO films as the third layer of the 3-SALs, we conducted the experiment with the mole ratio of In and Zn fixed at 5:2 and the Ga/(In + Ga + Zn) ratio varied at 0, 13, 30, and 42%. Figure 2a shows the transfer characteristics of the single active layer-based IGZO TFTs according to the change in the Ga mole ratio. When the Ga mole ratio increases, Ga suppresses the generation of oxygen vacancy, and the carrier concentration decreases, which decreases the on- and off-currents. In particular, as the Ga mole ratio increases, V_{TH} shifts in the positive direction, and μ_{FET} decreases, as shown in Figure 2b. Figure 2c shows the PBS reliability of the single active layer-based IGZO TFTs depending on the Ga mole ratio. As the Ga mole ratio increases, the TFT shows a highly stable behavior, which could be attributed to the reduction in oxygen vacancies and the defect densities related to oxygen vacancies.[14−16] To evaluate the time stability (increase in the off-current with time) of the IGZO TFTs, we kept them in an air environment for 148 h. As the Ga mole ratio increases, the off-current level gradually decreases, as shown in Figure 2d, attributed to the decrease in the conductivity in the IGZO film because of the reduction in the oxygen vacancies and the decrease in the defects related to the oxygen vacancies.[17,18]

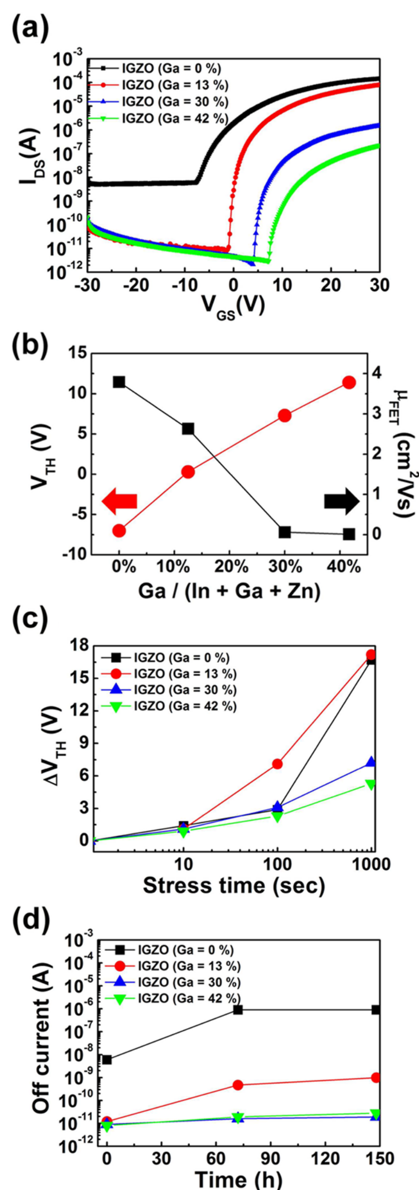

Figure 2. Electrical properties of the single active layer-based TFTs as a function of the Ga mole ratio. (a) Transfer characteristics. (b) V_{TH} and μ_{FET} characteristics. (c) ΔV_{TH} characteristics under PBS. (d) Change in the off-current with time (extracted at a V_G of 10 V).

We evaluated by XPS the change in the oxygen vacancies related to the oxygen deficiency because of the increase in the Ga mole ratio. Figure 3 shows the Gaussian fitted O1s peaks of the three regions centered at 529.8, 531.3, and 532.5 eV.[16] The low binding energy area (O_I) located at 529.8 eV indicates the O^{2-} ions associated with the neighboring metal ions. The

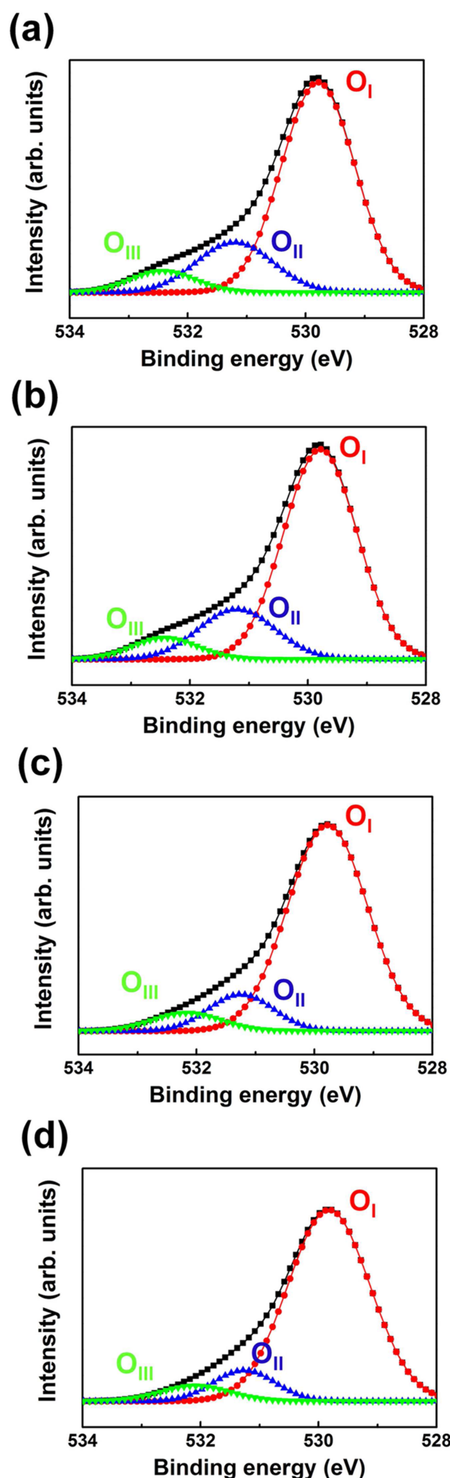

Figure 3. XPS results of the single IGZO film as a function of the Ga mole ratio. (a) IZO (Ga = 0%). (b) IGZO (Ga = 13%). (c) IGZO (Ga = 30%). (d) IGZO (Ga = 42%).

medium binding energy area (O_{II}) located at 531.3 eV indicates the oxygen-deficient regions. The high binding energy region (O_{III}) located at 532.5 eV indicates the loosely bound hydroxyl groups. We can predict the change in the oxygen vacancies from the area of the O_{II}/O_I region.[16] As the Ga mole ratio increases, the O_{II}/O_I area changes from 22.5 to 11.7%, attributed to the decrease in the oxygen vacancies owing to the higher attraction ability of the Ga ions than that of the In and/or Zn ions to oxygen ions. These results reflect the change in the electrical properties of the single active layer-based IGZO TFTs shown in Figure 2.

3.2. Electrical Characteristics of the 3-SAL IGZO TFTs with Self-Passivated Layer. Figure 2 shows that the single active layer-based IGZO TFTs has a relatively low μ_{FET} with the increase in the Ga mole ratio, whereas the PBS reliability and the time stability dramatically improve. Thus, we could expect the increase in the off-current in the air environment as well as the improvement in the PBS reliability by controlling the amount of Ga in the third layer of the 3-SALs because sufficient current could flow through the main channel region with the stacked active layers.[9] Further, the leakage current through the third layer at the back-channel region is prevented, as shown in Figure 4. To verify this SP-MSAL structure, the IGZO films were formed in the third layer, whose Ga/(In + Ga + Zn) ratio were varied as 0%, 13%, 30%, and 42%, and the first and the second layers were fixed with In, Ga, and Zn mole ratio of 5:1:2.[9]

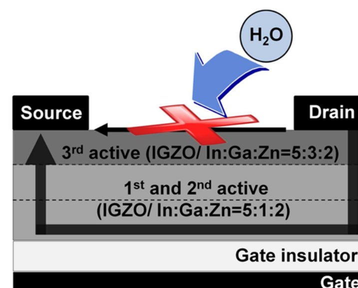

Figure 4. Schematic diagram of the SP-MSALs.

Figure 5a shows the transfer characteristics of the 3-SAL TFTs where the Ga mole ratio of the third layer is varied. Compared with the change in the electrical properties of the single active layer-based TFTs (Figure 2a), the 3-SAL TFTs have no apparent effect on V_{TH}, regardless of the Ga mole ratio in the third layer. Notably, the variation in μ_{FET} according to the Ga mole ratio in the third layer shows different behaviors as shown in Figure 5b. Improvement in μ_{FET} of the 3-SAL TFTs with a Ga/(In + Ga + Zn) ratio of 30% in the third layer was observed as compared with that with a Ga/(In + Ga + Zn) ratio of 0 and 13%. We believed that the improvement in μ_{FET} in the 3-SAL TFTs because of the reduction in the leakage current through the back channel under a high Ga mole ratio was more influential than the increased resistivity between the active and source−drain electrodes owing to the high resistivity in the third layer. However, μ_{FET} decreased when the Ga/(In + Ga + Zn) ratio was 42%. This result was not related to the interface properties because of the similar subthreshold swing (S.S) regardless of the Ga mole ratio, as shown in Figure 5b. Thus, it can be attributed to the high resistivity in the third layer. Therefore, we determined that the Ga/(In + Ga + Zn) ratio of 30% in the third layer is the optimal condition. Figure 5c shows the PBS reliability of the 3-SAL TFTs as a function of the Ga mole ratio in the third layer. As the Ga mole ratio in the third layer increased, the threshold voltage shift (ΔV_{TH}) reduced. Here, the carrier concentration of the third layer was low because of the suppression of the generation of oxygen vacancies caused by the addition of Ga. Thereby, the carrier concentration and trap density in the back-channel region was low. Accordingly, they contributed to the reduced leakage

dx.doi.org/10.1021/am4002259 | ACS Appl. Mater. Interfaces 2013, 5, 4190−4194

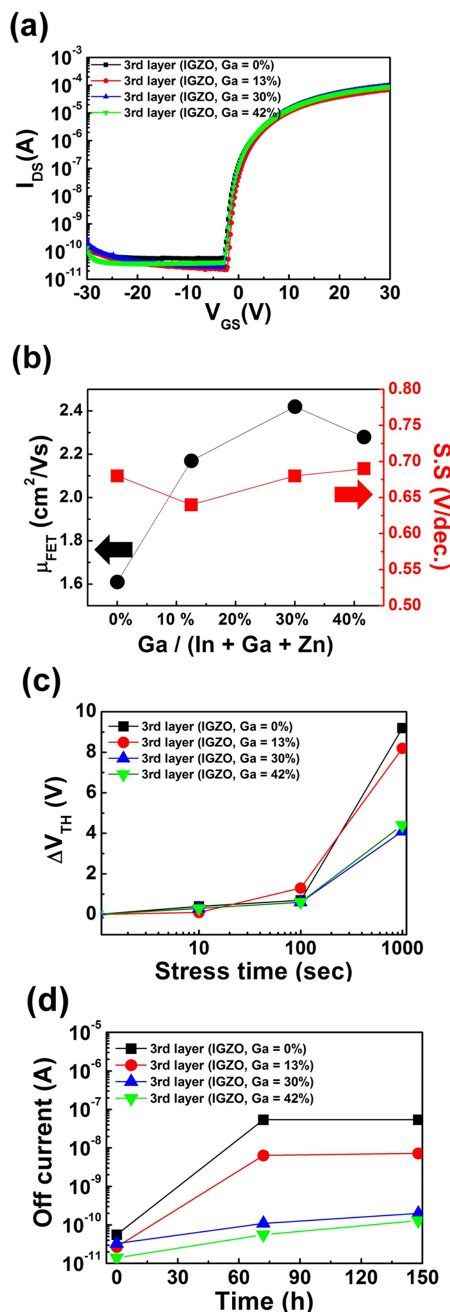

Figure 5. Electrical properties of the 3-SAL TFTs with a third layer as a function of the Ga mole ratio. (a) Transfer characteristics. (b) V_{TH} and S.S characteristics. (c) ΔV_{TH} characteristics under PBS. (d) Change in the off-current with time (extracted at a V_G of 10 V).

current in the back channel.[19−21] Figure 5d shows the variations in the off-current of the 3-SAL TFTs as a function of the exposure time in an ambient environment. Even though our device's back-channel region was exposed to the air environment, the change in the off-current in the 3-SAL TFTs was dramatically suppressed by the reduction in the oxygen vacancies with a high Ga mole ratio in the third layer. This result is similar to the formation of a protection layer (i.e., SiO_x or SiN_x layer) in the device to protect the electrical characteristics of the oxide semiconductor, which is sensitive to the air environment.[22] Therefore, the 3-SAL TFTs with layers with different atomic compositions could improve the PBS reliability and time stability.

4. CONCLUSION

The SP-MSAL structure has been applied to improve the features of the solution-processed IGZO TFTs. When the SP-MSAL TFTs are exposed to the air environment, this structure can effectively decrease the unexpected back-channel current in the exposed active layer because the carriers and the defects related to oxygen vacancies decrease by increasing the Ga content in the third layer of the SP-MSALs. The SP-MSALs have a bottom layer (the first and the second layers) where the current flows and a top layer (the third layer) that suppresses the back-channel effect. Accordingly, we confirmed that the SP-MSALs are effective structures to improve the PBS reliability and time stability.

AUTHOR INFORMATION

Corresponding Author

*E-mail: hjk3@yonsei.ac.kr.

Notes

The authors declare no competing financial interest.

ACKNOWLEDGMENTS

This work was supported by Samsung Display and the National Research Foundation of Korea (NRF) grant funded by the Korean Ministry of Education, Science and Technology (MEST) (2011-0028819).

REFERENCES

(1) Rim, Y. S.; Jeong, W. H.; Kim, D. L.; Lim, H. S.; Kim, K. M.; Kim, H. J. *J. Mater. Chem.* **2012**, *22*, 12491.
(2) Kim, Y.-H.; Heo, J.-S.; Kim, T.-H.; Park, S.; Yoon, M.-H.; Kim, J.; Oh, M. S.; Yi, G.-R.; Noh, Y.-Y.; Park, S. K. *Nature* **2012**, *489*, 128.
(3) Kim, M.-G.; Kanatzidis, M. G.; Facchetti, A.; Marks, T. J. *Nat. Mater.* **2011**, *17*, 382.
(4) Banger, K. K.; Yamashita, Y.; Mori, K.; Peterson, R. L.; Leedham, T.; Rickard, J.; Sirringhaus, H. *Nat. Mater.* **2010**, *10*, 45.
(5) Fortunato, E.; Barquinha, P.; Martins, R. *Adv. Mater.* **2012**, *24*, 2945.
(6) Mitzi, D. B. *Chem. Mater.* **2001**, *13*, 3283.
(7) Arai, T.; Morosawa, N.; Tokunaga, K.; Terai, Y.; Fukumoto, E.; Fujimori, T.; Nakayama, T.; Yamaguchi, T.; Sasaoka, T. *Dig. SID* **2010**, *41*, 1033.
(8) Li, C.-S.; Li, Y.-J.; Wu, Y.; Ong, B.-S.; Loutfy, R.-O. *J. Mater. Chem.* **2009**, *19*, 1626−1634.
(9) Kim, D. J.; Kim, D. L.; Rim, Y. S.; Kim, C. H.; Jeong, W. H.; Lim, H. S.; Kim, H. J. *ACS Appl. Mater. Interfaces* **2012**, *4*, 4001.
(10) Kang, D.; Lim, H.; Kim, C.; Song, I.; Park, J.; Chung, J.; Park, Y. *Appl. Phys. Lett.* **2007**, *90*, 192101.
(11) Nomura, K.; Ohta, H.; Takagi, A.; Kamiya, T.; Hirano, M.; Hosono, H. *Nature* **2004**, *432*, 488.
(12) Rim, Y. S.; Jeong, W.; Ahn, B. D.; Kim, H. J. *Appl. Phys. Lett.* **2013**, *102*, 143503.
(13) Nomura, K.; Ohta, H.; Ueda, K.; Kamiya, T.; Hirano, M.; Hosono, H. *Science* **2003**, *300*, 1269.
(14) Park, J.-S.; Kim, K.; Park, Y.-G.; Mo, Y.-G.; Kim, H. D.; Jeong, J. K. *Adv. Mater.* **2009**, *21*, 329.
(15) Kim, G. H.; Jeong, W. H.; Ahn, B. D.; Shin, H. S.; Kim, H. J.; Ryu, M.-K.; Park, K.-B.; Seon, J.-B.; Lee, S.-Y. *Appl. Phys. Lett.* **2010**, *96*, 163506.
(16) Jeong, Y.; Song, K.; Jun, T.; Jeong, S.; Moon, J. *Thin Solid Films* **2011**, *519*, 6164.
(17) Jeong, J. K.; Yang, H. W.; Jeong, J. H.; Mo, Y.-G.; Kim, H. D. *Appl. Phys. Lett.* **2008**, *93*, 123508.
(18) Lee, K.-H.; Jung, J. S.; Son, K. S.; Park, J. S.; Kim, T. S.; Choi, R.; Jeong, J. K.; Kwon, J.-Y.; Koo, B.; Lee, S. *Appl. Phys. Lett.* **2009**, *95*, 232106.

(19) Son, K.-S.; Kim, T.-S.; Jung, J.-S.; Ryu, M.-K.; Park, K.-B.; Yoo, B.-W.; Park, K.; Kwon, J.-Y.; Lee, S.-Y.; Kim, J.-M. *Electrochem. Solid State Lett.* **2009**, *12*, H26−H28.
(20) Tsai, C.-T.; Chang, T.-C.; Chen, S.-C.; Lo, L.; Tsao, S.-W.; Hung, M.-C.; Chang, J.-J.; Wu, C.-Y.; Huang, C.-Y. *Appl. Phys. Lett.* **2010**, *96*, 242105.
(21) Liu, P.-T.; Chou, Y.-T.; Teng, L.-F.; Li, F.-H.; Shieh, H.-P. *Appl. Phys. Lett.* **2011**, *98*, 052102.
(22) Park, J. S.; Kim, T. S.; Son, K. S.; Lee, K.-H.; Maeng, W.-J.; Kim, H.-S.; Kim, E. S.; Park, K.-B.; Seon, J.-B.; Choi, W.; Ryu, M. K.; Lee, S. Y. *Appl. Phys. Lett.* **2010**, *96*, 262109.